EurJIC
European Journal of Inorganic Chemistry

A Journal of ChemPubSoc Europe

Accepted Article

Title: An all-in-one molecule for the one-step synthesis of functional hybrid silica particles with tunable size

Authors: Julien Graffion, Dounia Dems, Mesut Demirelli, Thibaud Coradin, Nicolas Delsuc, and Carole Aimé

To be cited as: *Eur. J. Inorg. Chem.* 10.1002/ejic.201701181

Link to VoR: http://dx.doi.org/10.1002/ejic.201701181

WILEY-VCH

WILEY-VCH

COMMUNICATION

An all-in-one molecule for the one-step synthesis of functional hybrid silica particles with tunable size

Julien Graffion,[a,b] Dounia Dems,[a,b] Mesut Demirelli,[a,b] Thibaud Coradin,[a,b] Nicolas Delsuc,[c] and Carole Aimé*[a,b]

Abstract: Spherical particles with well-defined diameters are obtained by self-assembly of trityl-based molecules. Thanks to the robustness of the organic scaffold, a variety of modifications can be covalently introduced into the network so as to stabilize the supramolecular structure by a sol-gel route. Using supramolecular chemistry, we show that the synthesis of hybrid small molecules allows engineering nanomaterials with tunable size and functionality. The use of a combination of different characterization techniques including dynamic light scattering, cryoTEM and solid-state NMR provides a careful understanding of the relationship between molecular and supramolecular structures for further chemical engineering of supramolecular hybrid materials.

Anti-solvent precipitation is an attractive technique for the elaboration of nanoparticles (NPs) finding applications in various fields such as electro-optics, catalysis, and nanomedicine notably with the elaboration of imaging agents and for improving drug formulation. Alternatively, the design and synthesis of nanoscale metal-organic frameworks have provided tunable nanoobjects to serve as functional platforms.[1-6] However, despite the size tunability of the resulting particles, their high interfacial area renders them prone to aggregation and Oswald ripening that affect their stability.[7] Research efforts have been devoted to the selection of stabilizers to be added to the precipitating nanoparticles.[8] To this aim, amphiphilic diblock copolymers have been used, typically a hydrophilic poly(ethylene glycol) (PEG) block chemically linked to a hydrophobic block.[9] Thanks to its amphiphilic properties, the polymer adsorbs at the surface of the NPs limiting further growth or dissolution, and preventing aggregation. Polyelectrolytes such as polylysine, poly(ethylene imine) or chitosan have also been used to electrostatically and sterically stabilize the NPs and ensure narrow size distribution.[10] Alternatively, hybrid (organic-inorganic) materials have been intensively investigated for two decades due to their unique properties that combine hardness and stability of the inorganic phase with the flexibility and mild processing of polymer materials.[11,12] As recently reviewed,[13] silsesquioxane NPs have been synthesized from organotrialkoxysilane precursors by different routes including hydrolytic[14-17] and non-hydrolytic[18] sol-gel routes, and emulsion polymerization.[19-22] With such processes, spherical,[14,15,23-25] hollow,[26-30] and Janus[31] NPs can be obtained. Their surface can be easily functionalized through silanization reactions of superficial silanol groups.[32,33] This offers a large number of possibilities to bind targeting moieties for imaging or drug delivery systems[34] or enhance cell compatibility and internalization.[35,36]

Among polysilsesquioxanes, phenylsilsesquioxanes have drawn much attention, and synthesis of $PhSiO_{3/2}$ particles reported.[16,37] In another study, Dirè et al synthesized NPs from a series of alkyltriethoxysilane (methyl-, ethyl-, vinyl-, phenyl-, amyl- and octyltriethoxysilane) with a systematic assessment of the influence of the different organic groups on the synthesis and properties of silsesquioxane NPs.[25] Such molecular design may allow the doping of particles, either by physical entrapment or covalent linking, with representative examples using fluorophores such as Nile red,[38] rhodamine B,[17,24,39] or rhodamine 6G.[25] It is worth mentioning that for the above-cited alkyltriethoxysilanes, the formation of nanoparticles results from nucleation and growth induced by sol-gel polymerization, typically following a two-steps hydrolysis-condensation process as in the case of Dirè et al works. On the other hand, the self-assembly of silsesquioxanes has been reported for the design of helical or lamellar structures with organogelator-like behavior.[40-42]

In this work, we exploit the supramolecular interaction properties of the organic moiety of organotrialkoxysilanes as the only molecular key towards nanoparticles. We use different molecular designs based on triphenylmethane (trityl) group (Figure 1) to take advantage of the trityl moiety to drive the formation of well-defined objects. The addition of a trialkoxysilane group (2 Figure 1) aims at allowing their stabilization through sol-gel chemistry, preventing aggregation and Oswald ripening. Finally, in order to investigate the scope of the tolerated modifications that preserve the structure of the objects, we have introduced a chiral multifunctional backbone that is a L cystein amino acid. Its thiol group has been functionalized with the trityl group as for 1 and 2 and the trialkoxysilane has been introduced

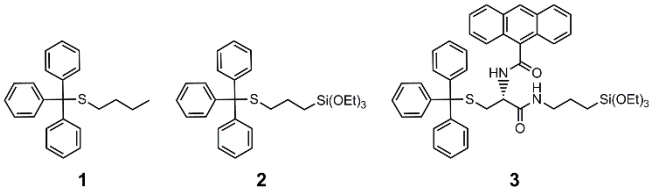

1 2 3

Figure 1. Molecular structures synthesized from an alkyl-S-trityl moiety (1), combining a triethoxysilane group (2), and belonging to a cystein functionalized with an anthracene (3).

[a] Dr. J. Graffion, D. Dems, M. Demirelli, Dr. T. Coradin, Dr. C. Aimé
Sorbonne Universités, UPMC Univ Paris 06, Collège de France, UMR CNRS 7574, Laboratoire de Chimie de la Matière Condensée de Paris, Paris cedex 05, France.
E-mail: carole.aime@upmc.fr
[b] Dr. J. Graffion, D. Dems, M. Demirelli, Dr. T. Coradin, Dr. C. Aimé
PSL Research University
[c] Dr. N. Delsuc
Laboratoire des Biomolécules, Département de chimie, École normale supérieure, PSL Research University, Sorbonne Universités, UPMC Univ. Paris 06, CNRS, 24 rue Lhomond, 75005 Paris, France.

Supporting information for this article is given via a link at the end of the document.

10.1002/ejic.201701181

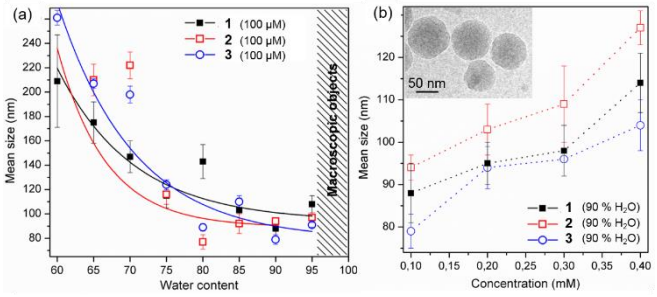

Figure 2. DLS of the supramolecular structures of 1, 2, and 3 as a function of (a) water content (100 µM), and (b) concentration (90 % water). Inset cryoTEM of 3 (200 µM, 90 % water).

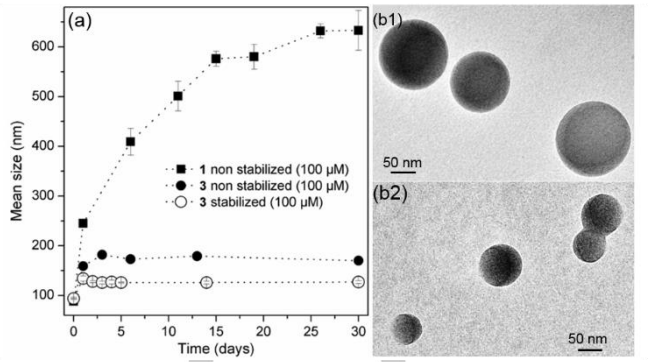

Figure 3. (a) DLS of the supramolecular structures obtained from 1 and 3 with (stabilized) or without (non-stabilized) ammonia vapors and (b) TEM images of the stabilized spheres obtained from 2 and 3 respectively (90 % water, 100 µM).

via a DCC/NHS coupling with (3-aminopropyl)triethoxysilane (APTES). A fluorescent anthracene moiety has been conjugated to the amine function of the cystein. This provides cues for a functional implementation of the resulting supramolecular structures in an "all-in-one molecular structure" (3 Figure 1). The three molecules have been synthesized as described in schemes S1 and S2 and were obtained with a high purity (> 95 %, no detectable impurities by 1H NMR).

Antisolvent precipitation in an ethanol/water mixture was used to obtain supramolecular objects from 1. Precipitation could be monitored by dynamic light scattering (DLS) in the range 60 to 95 % water leading to well-defined objects with sizes from 210 nm to ca. 100 nm (Figure 2a). No supramolecular structure could be detected below this range due to the solubility of 1 in ethanol, while macroscopic objects sedimented above 95 % water. Very interestingly, similar trends could be observed by precipitating 2 and 3, with a constant decrease in size from 60 to 80 % water giving rise to well-defined objects with a mean hydrodynamic diameter above 200 nm at 60 % (210 nm for 1, 260 nm for 3) levelling around 90 nm from 80 to 95 % water. It is worth mentioning that as the water content increases the size distribution becomes narrower (Table S1). Playing with the tritylated molecule concentration at a given water content is an additional way of tuning the size of the resulting supramolecular structures. At 90 % water, when increasing the alkoxysilane concentration from 100 to 400 µM, the hydrodynamic diameter of 2 can be steadily varied from 95 to 125 nm, and from 80 to 100 nm for 3 (Figure 2b). CryoTEM observations show the formation of well-defined spherical objects in solution (Figure 2B, inset). Overall, the precipitation of 1 and the similar trends observed with 2 and 3 show that the strong hydrophobic character and the non-planar structure (one sp3 carbon) of trityl favor pi-stacking interactions over a short range, which makes it particularly interesting for antisolvent precipitation to obtain well-defined spherical objects. Trityl assembly being the driving force for the formation of spherical particles, its scaffolding role is strong enough to ensure particle formation upon addition of even large organic molecules. Interestingly, neither the alkoxysilane, nor the chiral centre and anthracene moiety seemed to play an important role for obtaining well-defined nanostructures since 1, 2 and 3 behaved similarly. In presence of a chiral center, the preservation of a chiral environment within hybrid particle could be ascertained by circular dichroism spectropolarimetry (Figure S3). Because this supramolecular chirality is expressed without modifying any of the previously described characteristics of the nanomaterials, this process is very tolerant to a wide range of modifications.

The introduction of the alkoxysilane group may offer a way of stabilizing the supramolecular particles of 2 and 3. Indeed, the size of objects from 1 increases progressively up to 633 ± 40 nm after one month (Figure 3a). In the case of precursors 2 and 3, after the nanoparticles formation, a sol-gel route was used by placing the samples under ammonia vapors for 24 h to catalyze their hydrolysis-condensation under basic conditions. For example, in the case of 3, after this treatment, the size of the spheres levels at 127 ± 3 nm after 1 day, while in absence of ammonia stable spherical structures could be obtained after 3 days exhibiting a size of 170 ± 7 nm. This shows (i) the role of the alkoxysilane moiety in the stabilization of the final structures and (ii) that ammonia is not mandatory for the stabilization of 3 but speeds up the kinetics of the sol-gel process. TEM observations after stabilization of 2 and 3 showed the preservation of the spherical structures (Figure 3b). In terms of chemical structure, the hydrolysis-condensation of the alkoxysilane and the formation of the siloxane shell at the surface were ascertained using Zeta potential measurements and 29Si solid state NMR. Stabilized particles from 2 and 3 show negative zeta potentials indicative of the presence of silanolate groups, resulting from the hydrolysis of ethoxysilanes, on their surface (Table S2). Probing the silicon chemical environment of 3 after stabilization by 29Si NMR showed broad signals around -45.4, -57.1 and -66.8 ppm attributed respectively to R-Si(OEt)3, R-Si(OSi)2(OH) (T2) and R-Si(OSi)3 (T3), which confirm partial alkoxysilane condensation (Figure S1). Further investigations by FTIR show that the Si-O deformation region (900-1145 cm-1) does not change when comparing 3 as molecular precursor and as stabilized particles (Figure S2). In addition, no condensed siloxane bond (vas (SiOSi)) could be identified due to their low concentration, restricted to the surface. These results provide evidences that the precursor remains intact within the nanoparticles due to the hydrophobic character of the core that prevents water and ammonia internal diffusion. Further investigations using powder X-ray diffraction (PXRD) showed the presence of amorphous silica, which could be expected given the huge number of molecules involved in the formation of 100 nm diameter particles (Figure S4).

As a mean of implementing the particle with functionality, a fluorescent probe, namely an anthracene, was introduced to the

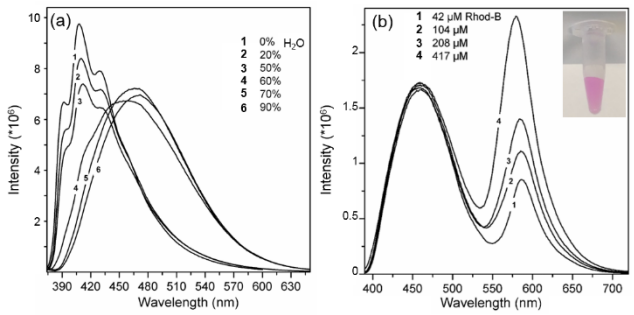

Figure 4. Emission spectra of 3 (a) as a function of water content (100 µM, λexc 375 nm), and (b) after rhod-B addition at different concentrations ([3] 200 µM, 90 % water, λexc 378 nm).

molecular design (3). The covalent conjugation of the anthracene probe allows preventing the fluorophore leaching. Figure 4a shows the emission spectra of 3 with increasing water content up to 90 %. From 0 to 50 % water, the emission of the anthracene (well-defined components, maximum intensity at 407 nm) indicates that the anthracene moiety exists as a monomer in solution. From 60 to 90 % water, the emission spectra drastically broaden and red-shift (maximum intensity around 470 nm). These changes are attributed to the transition from soluble 3 to its precipitated state, in good agreement with DLS measurements where no supramolecular structure could be detected below 60 % water. As expected, the excitation spectrum was also slightly red-shifted (7 nm) with increasing water content (Figure S5a).

Since 3 was shown to be an efficient multifunctional scaffold to form hybrid nanoparticles with easily tunable diameters, we investigated further the possibility to increase their functionality by physical encapsulation. As a proof of concept, the encapsulation ability of the hybrid particles was assessed by the addition of rhodamine-B (rhod-B) during the precipitation of 3. Rhod-B was chosen to get insights into the impact of adding sizeable molecules on the stability and size of the hybrid particles. In addition, rhod-B was selected because it provides a straightforward read-out of the encapsulation, using Förster Resonance Energy Transfer (FRET) with the anthracene moiety. Different concentrations of rhod-B were added during the precipitation of 3 (200 µM, 90 % water). After stabilization and removal of non-encapsulated dye upon centrifugation, a pink precipitate consisting of hybrid particles incorporating rhod-B could be recovered and further redispersed in water (Figure 4b inset). DLS measurements showed an increase in size from 90 nm to ca. 160 nm upon rhod-B encapsulation while no variation in zeta potential could be detected, signing for dye encapsulation rather than surface adsorption (Table S3,S4). A photoluminescence study was performed to provide additional evidence of the encapsulation of rhod-B in stabilized hybrid particles of 3. Emission spectra recorded at an excitation wavelength in the anthracene region (378 nm) allowed the detection of emissions of both the anthracene (centered at 460 nm) and rhod-B (at 580 nm) through FRET (Figure 4b). Excitation spectra recorded at the maximum intensity of rhod-B emission (λem 587 nm) also show the contribution of the anthracene moiety in 3, which confirms the FRET phenomenon between rhod-B and 3, further evidencing the encapsulation of rhod-B (Figure S5b). Noteworthy, the emission intensity of rhod-B increases with its initial concentration, while the emission intensity of 3 remains constant (Figure 4b). The ratio of the emission band area of rhod-B over 3 rapidly increases with rhod-B concentration before it starts to level off around 2 mM, which may indicate that saturation is approaching (Figure S6). The saturation regime could not be investigated further due to the destruction of hybrid particles at higher rhod-B concentrations. Importantly, up to 2 mM rhod-B, the integrity of the particles could be preserved (Figure S7). These results show the robustness of the molecular design, where stable spherical nanoparticles could still be obtained even after addition of rhod-B.

In conclusion, spherical nanoparticles with well-defined tunable diameters could be obtained in a single step by antisolvent precipitation. Our “all-in-one molecule” is based on an organic moiety, trityl, which is solely responsible for nanoparticles formation. The addition of an alkoxysilane group allows the stabilization of the hybrid particles by hydrolysis and condensation, to freeze the final system and avoid further shape and size evolution. We show that the propensity of the trityl group to generate supramolecular spheres provides this molecular design with a unique robustness that allows the covalent introduction of large organic groups without changing the structural properties of the particles. This opens the doors towards a broad range of functional implementations as illustrated by the covalent conjugation of fluorophores. In addition, such nanoparticles allow the encapsulation of large molecules without modifying their structure, which indeed opens up additional opportunities. Finally, we have to keep in mind that the functionality of those nanoparticles could even be broaden given the versatility of silane chemistry for further functionalization of the nanoparticles surface, in particular when envisioning applications in biotechnologies and nanomedicine.

Experimental Section

Preparation of 1, 2 and 3 hybrid nanoparticles

Solutions of 1, 2 or 3 in ethanol were quickly added onto freshly deionized water under vigorous stirring (always the same speed) at room temperature for 30 seconds. For each precursor, water-ethanol ratio (from 0% to 95% water) and concentration (100, 200 and 400 µM), the final volume was always kept at 1.5 mL for reproducibility reasons.

For non-stabilized systems, the suspension was left without further stirring. For the stabilized, the suspension was placed in sealed environment for 24h in presence of ammonia vapours followed by 48h of ageing in the newly basified suspension through ammonia transfer.

To recover the stabilized hybrid nanoparticles, centrifugations and cycle of washing, with a mixture of ethanol-deionized water 1:1 first then with deionized water (4 times), were used.

Preparation of 3 hybrid nanoparticles containing rhodamine-B

Solutions of 3 in ethanol were quickly added onto solutions of freshly deionized water (90% water content in all cases) containing 0.2 (42 µM), 0.5 (104 µM), 1 (208 µM), 2 (417 µM), 5 (834 µM) or 10 mg (2080 µM) of rhodamine-B. The conditions of stirring, temperatures, volumes, stabilizations and washing were the same than for the preparation of 3 hybrid Nanoparticles (see above). Although in this case, the final concentration of 3 was kept at 200 µM only.

Dynamic light scattering (DLS) and zeta potential measurements

Zeta potential and size distribution measurements were carried out using a Malvern Zetasizer Nano ZS90 instrument. The autocorrelation functions

were recorded at a scattering angle θ = 90o and analyzed by the non-negatively constrained least squares technique (NNLS-Multiple Pass) for the determination of particles diameter. All the suspensions were sonicated for 5 seconds prior measurement at 20°C. For DLS measurements, all measurements were run in triplicate to obtain the size standard deviation.

Transmission electron microscopy

A drop of sample in aqueous solution (7 µl) was deposited on carbon-coated copper grids (400 mesh, Electron Microscopy Sciences). After 3 minutes, the excess liquid was blotted with filter paper (Whatman #4). TEM was performed at RT using a FEI Technai Spirit G2 operating at 120 kV. Images were recorded on a Gatan Orius CCD camera.

Fluorescence spectroscopy

Fluorescence measurements were recorded on a Fluoromax-3 (Horiba Jobin Yvon Perkin Elmer LS55) spectrometer, with a 150-W ozone-free xenon arc-lamp as excitation source. Emission spectra (350-650 nm for 3, and 390-725 nm for rhodamine B @ 3) were recorded with excitation wavelength of 375 and 378 nm in absence and presence of rhodamine B respectively. The bandpass of the excitation and emission monochromators was set at 5 nm, and the scan speed at 10 nm/sec. Samples were investigated at 25 °C in 1 cm path length cells.

Acknowledgements

The authors thank Clément Sanchez, François Ribot and Cédric Boissière for fruitful discussions, Gervaise Mosser for cryoTEM observations and careful reading of the manuscript, Patrick le Griel for his help in electron microscopy, Cristina Coelho-Diogo for solid-state NMR, Mohamed Selmane for PXRD experiments, the CNRS and the Idex PSL ANR-10-IDEX-0001-02 PSL for funding.

Keywords: hybrid nanoparticles • supramolecular assembly • alkoxysilane

[1] W. Cai, C.-C. Chu, G. Liu, Y.-X. J. Wáng, Small, 2015, 11, 4806-4822.
[2] J. Della Rocca, D. Liu, W. Lin, Acc Chem Res., 2011, 44, 957-968.
[3] A. Carné, C. Carbonell, I. Imaz, D. Maspoch, Chem. Soc. Rev., 2011, 40, 291–305.
[4] R.-R. Gao, S. Shi, Y.-J. Li, M. Wumaier, X.-C. Hu, T.-M. Yao, Nanoscale, 2017, 9, 9589–9597.
[5] H.-H. Zeng, W.-B. Qiu, L. Zhang, R.-P. Liang, J.-D. Qiu, Anal. Chem. 2016, 88, 6342-6348.
[6] C. Aimé, R. Nishiyabu, R. Gondo, N. Kimizuka, Chem. Eur. J., 2010, 16, 3604-3607.
[7] Y. Liu, K. Kathan, W. Saad, R. K. Prud'homme, *Phys. Rev. Lett.,* **2007**, *98*, 036102.
[8] W. S. Saad, R. K. Prud'homme, *Nano Today,* **2016**, *11*, 212-227.
[9] Z. Zhu, *Biomaterials,* **2013**, *34*, 10238-10248.
[10] Z. Zhu, K. Margulis-Goshen, S. Magdassi, Y. Talmon, C. W. Macosko, *J. Pharm. Sci.,* **2010**, *99*, 4295-4306.
[11] A. P. Wight, M. E. Davis, *Chem. Rev.,* **2002**, *102*, 3589-3614.
[12] C. Sanchez, B. Lebeau, F. Chaput, J.-P. Boilot, *Adv. Mater.,* **2003**, *15*, 1969-1994.
[13] J. G. Croissant, X. Cattoën, J.-O. Durand, M. Wong Chi Man, N. M. Khashab, *Nanoscale,* **2016**, *8*, 19945-19972.
[14] A. Arkhireeva, J. N. Hay, *J. Mater. Chem.,* **2003**, *13*, 3122-3127.
[15] M. Nakamura, K. Ishimura, *J. Phys. Chem. C*, **2007**, *111*, 18892-18898.
[16] J. Macan, K. Tadanaga, M. Tatsumisago, *J. Sol-Gel Sci. Technol.,* **2010**, *53*, 31-37.
[17] M. Nakamura, K. Ishimura, *Langmuir,* **2008**, *24*, 5099-5108.
[18] A. Arkhireeva, J. N. Hay, *Chem. Mater.*, **2005**, *17*, 875-880.
[19] A. Arkhireeva, J. N. Hay, W. Oware, *J. Non-Cryst. Solids,* **2005**, *351*, 1688-1695.
[20] I. Noda, T. Kamoto, M. Yamada, *Chem. Mater.*, **2000**, *12*, 1708-1714.
[21] F. Baumann, M. Schmidt, B. Deubzer, M. Geck, J. Dauth, *Macromolecules*, **1994**, *27*, 6102-6105.
[22] I. Noda, M. Isikawa, M. Yamawaki, Y. Sasaki, *Inorg. Chim. Acta*, **1997**, *263*, 149-152.
[23] A. Arkhireeva, J. N. Hay, J. M. Lane, M. Manzano, H. Masters, W. Oware, S. J. Shaw, *J. Sol-Gel Sci. Technol.*, **2004**, *31*, 31-36.
[24] M. Nakamura, K. Hayashi, M. Nakano, T. Kanadani, K. Miyamoto, T. Kori, K. Horikawa, *ACS Nano*, **2015**, *9*, 1058-1071.
[25] S. Dirè, V. Tagliazucca, E. Callone, A. Quaranta, *Mater. Chem. Phys.,* **2011**, *126*, 909-917.
[26] X. Li, Y. Yang, Q. Yang, *J. Mater. Chem. A*, **2013**, *1*, 1525-1535.
[27] Q. Wang, Y. Liu, H. Yan, *Chem. Commun.*, **2007**, 2339-2341.
[28] F. Dong, W. Guo, S.-W. Chu, C.-S. Ha, *Chem. Commun.*, **2010**, *46*, 7498-7500.
[29] F. Dong, W. Guo, S.-S. Park, C.-S. Ha, *J. Mater. Chem.*, **2011**, *21*, 10744-10749.
[30] Y. Xing, J. Peng, K. Xu, W. Lin, S. Gao, Y. Ren, X. Gui, S. Liang, M. Chen, *Chem. Eur. J.*, **2016**, *22*, 2114-2126.
[31] H. Ujiie, A. Shimojima, K. Kuroda, *Chem. Commun.*, **2015**, *51*, 3211-3214.
[32] P. Horcajada, A. Rámila, G. Férey, M. Vallet-Regí, *Solid State Sci.*, **2006**, *8,* 1243-1249.
[33] A. Liberman, N. Mendez, W. C. Trogler, A. C. Kummel *Surf. Sci. Rep.*, **2014**, *69*, 132-158.
[34] P. Yang, S. Gaib, J. Lin, *Chem. Soc. Rev.*, **2012**, *41*, 3679-3698.
[35] D. Kumar, I. Mutreja, P. C. Keshvan, M. Bhat, A. K. Dinda, S. Mitra, *J. Pharm. Sci.*, **2015**, *104*, 3943-3951.
[36] N. Ornelas-Soto, R. Rubio-Govea, C. E. Guerrero-Beltrán, E. Vázquez-Garza, J. Bernal-Ramírez, A. García-García c, Y. Oropeza-Almazán, G. García-Rivas, F. F. Contreras-Torres, *Mater. Sci. Eng. C*, **2017**, *79*, 831-840.
[37] H. J. Hah, J. S. Kim, B. J. Jeon, S. M. Koo, Y. E. Lee, *Chem. Commun.*, **2003**, 1712-1713.
[38] J. Qian, X. Li, M. Wei, X. Gao, Z. Xu, S. He, *Opt. Express*, **2008**, *16*, 19568-19578.
[39] R. Kumar, I. Roy, T. Y. Hulchanskyy, L. N. Goswami, A. C. Bonoiu, E. J. Bergey, K. M. Tramposch, A. Maitra, P. N. Prasad, *ACS Nano*, **2008**, *2*, 449-456.
[40] J. J. E. Moreau, L. Vellutini, M. Wong Chi Man, C. Bied, *J. Am. Chem. Soc.* **2001**, *123*, 1509-1510.
[41] J. J. E. Moreau, L. Vellutini, M. Wong Chi Man, C. Bied, P. Dieudonné, J.-L. Bantignies, J.-L. Sauvajol, Chem. Eur. J. 2005, 11, 1527-1537.
[42] A. Shimojima, Z. Liu, T. Ohsuna, O. Terasaki, K. Kuroda, J. Am. Chem. Soc. 2005, 127, 14108-14116.

10.1002/ejic.201701181

WILEY-VCH

Entry for the Table of Contents (Please choose one layout)

Layout 1:

COMMUNICATION

Spherical particles with well-defined diameters are obtained by self-assembly of trityl-based molecules. Thanks to the robustness of the organic scaffold, a variety of modifications can be covalently introduced into the network. Using supramolecular chemistry, we show that the synthesis of hybrid small molecules allows engineering nanomaterials with tunable size and functionality.

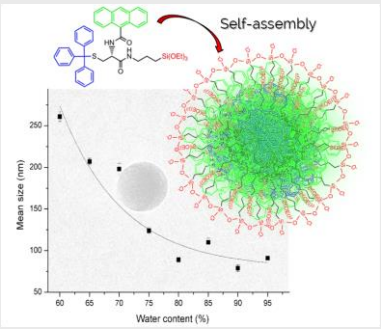

*Julien Graffion, Dounia Dems, Mesut Demirelli, Thibaud Coradin, Nicolas Delsuc, Carole Aimé**

Page No. – Page No.

An all-in-one molecule for the one-step synthesis of functional hybrid silica particles with tunable size

Layout 2:

COMMUNICATION

((Insert TOC Graphic here))

Page No. – Page No.

Text for Table of Contents